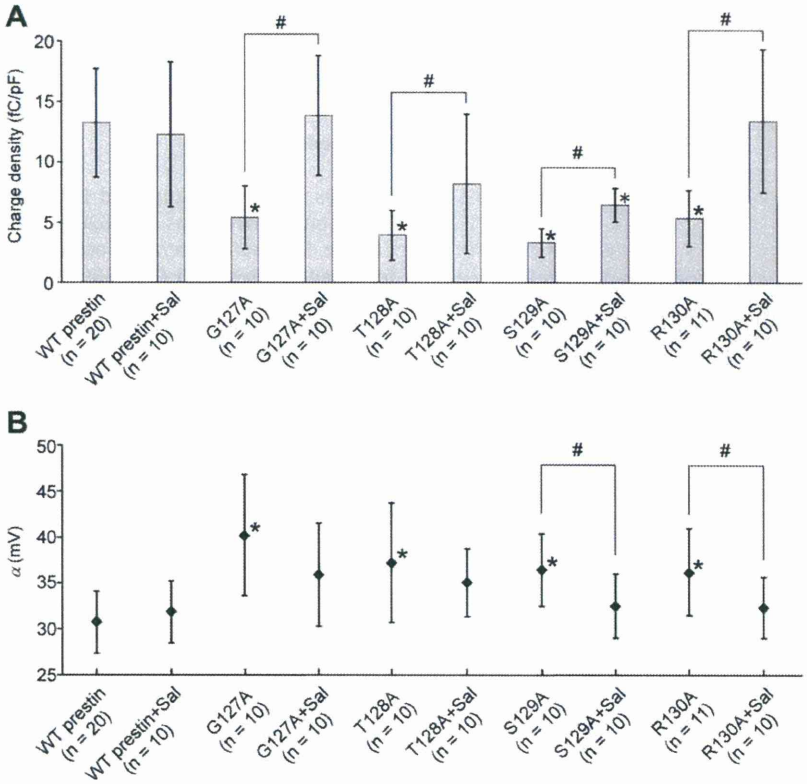

Fig. 4. Changes in the charge density and α of prestin by salicylate. (A) Charge density. The charge density of WT prestin was not affected by salicylate. On the other hand, the charge densities of G127A+Sal, T128A+Sal, S129A+Sal and R130A+Sal were statistically larger than those of G127A, T128A, S129A and R130A, respectively. (B) α. Without salicylate, the α values of G127A, T128A, S129A and R130A were statistically different from that of WT prestin. On the other hand, when 10 mM salicylate was used, there was no statistical difference in the α between the prestin mutants and WT prestin. Asterisks show the statistical differences in the charge density and α between WT prestin and the prestin mutants and between WT prestin+Sal and the prestin mutants+Sal ($p < 0.05$). Number signs indicate statistical differences in the charge density and α between cells cultured with salicylate and those cultured without it in each prestin mutant ($p < 0.05$). Error bars represent standard deviations.

prestin. On the other hand, the charge densities of G127A+Sal, T128A+Sal, S129A+Sal and R130A+Sal were statistically larger than those of G127A, T128A, S129A and R130A, respectively ($p < 0.05$). Especially, the charge density of G127A+Sal and that of R130A+Sal were similar to that of WT prestin+Sal. These results indicate that the charge density of those four mutants was recovered due to salicylate. On the other hand, H131A and S129T did not show NLC even when transfected cells were cultured with 10 mM salicylate.

The α was considered to represent properties of the anion binding of prestin [15]. Such values of G127A, T128A, S129A and R130A were statistically different from that of WT prestin when salicylate was not used (Fig. 4). On the other hand, when transfected cells were cultured with 10 mM salicylate, there was no statistical difference in α between the prestin mutants and WT prestin (Fig. 4). These results may imply that culturing the cells with salicylate somehow affects the properties of the anion binding of prestin.

3.3. Correlation between the R_p and the charge density

Without salicylate, the R_p values of all prestin mutants were lower than that of WT prestin. In this condition, the charge density of the prestin mutants was also lower or not recorded. On the other hand, salicylate increased both R_p and the charge density of G127A, T128A, S129A and R130A. Especially in G127A and R130A, R_p as well as the charge density recovered to the WT prestin level. This trend suggests that the changes in the charge density were correlated with changes in the R_P. Although R_p increased to some degree due to the addition of salicylate, H131A and S129T did not show NLC, possibly indicating that the amount of those mutants in the plasma membrane was still insufficient for detection of NLC. Another possibility is that H131A and S129T were promoted to be expressed in the plasma membrane but were non-functional.

Regarding S129A and S129T, the replacement of Ser-129 by threonine affected both the R_p and the charge density of prestin more strongly than that by alanine. Alanine and threonine are, respectively, smaller and larger than serine. Thus, the existence of an amino acid larger than serine at position 129 of prestin may be a steric constraint, affecting its characteristics significantly.

3.4. Changes in the concentration of salicylate

Salicylate at the concentration of 10 mM was found to recover the plasma membrane expression and the charge density of G127A and R130A to the WT prestin level as described above. Effects of decreasing the concentration of salicylate from 10 mM to 5 mM and 1 mM on the promotion of the plasma membrane expression were then evaluated using the cells transfected with R130A. Confocal images of the stained cells and calculated R_p are shown in Fig. 5A and B, respectively. The R_p of R130A was unchanged by 1 mM salicylate, while it was increased by 5 mM salicylate but not to the WT prestin level, suggesting that the promotion by salicylate of the plasma membrane expression of prestin mutants was concentration-dependent.

3.5. Discovery of new effect of salicylate on prestin

Salicylate is generally known to be an antagonist of prestin [8,9]. In the present study, another feature of salicylate was

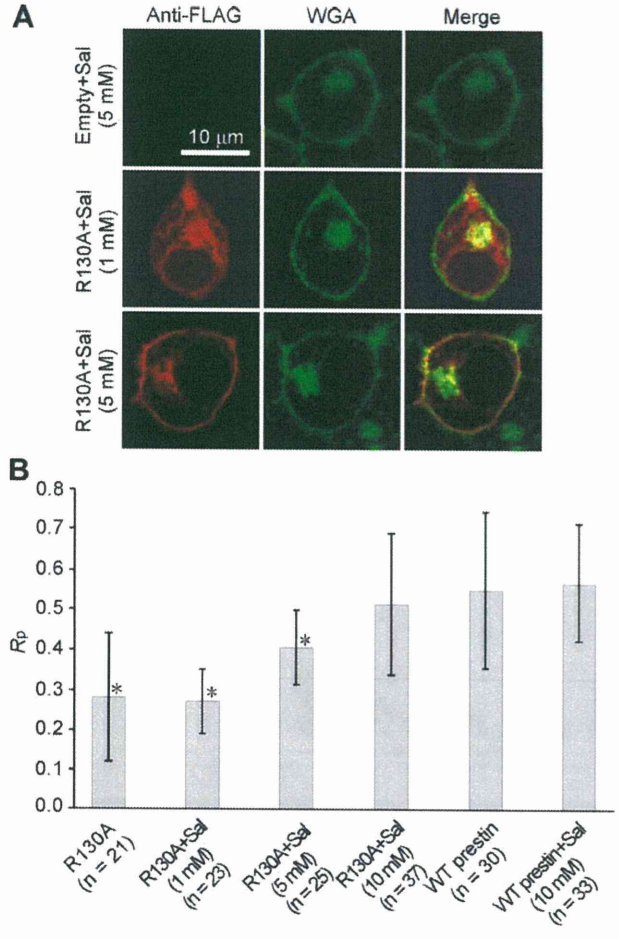

Fig. 5. Concentration dependence of the effects of salicylate on the localization of prestin. (A) Confocal microscopy images of stained cells. (B) Difference in the R_p due to the difference in the concentration of salicylate. The samples of R130A-expressing cells cultured without salicylate, with 1 mM salicylate, with 5 mM salicylate and with 10 mM salicylate are termed R130A, R130A+Sal (1 mM), R130A+Sal (5 mM) and R130A+Sal (10 mM), respectively, in this figure. In addition, the samples of WT prestin-expressing cells cultured without salicylate and with 10 mM salicylate are termed WT prestin and WT prestin+Sal (10 mM), respectively. The R_p of R130A was unchanged by 1 mM salicylate, but was increased by 5 mM salicylate. When transfected cells were cultured with 10 mM salicylate, the R_p recovered to the WT prestin level. Asterisks represent significance vs. WT prestin+Sal (10 mM) ($p < 0.05$). Error bars indicate standard deviations.

discovered, namely, it can promote the plasma membrane expression of prestin mutants accumulated in the cytoplasm, resulting in the recovery of the charge density. Various research findings have reported that if membrane proteins were accumulated in the cytoplasm due to their misfolding, a pharmacological chaperone bound to these proteins and then promoted their correct folding, resulting in their plasma membrane expression [3–7]. These reports may lead to a speculation that the prestin mutants analyzed in the present study were misfolded in the cytoplasm and that salicylate bound to these mutants and then induced their correct folding, promoting their transport to the plasma membrane. The next step of our study is to clarify if such speculation is correct, namely, to investigate the mechanism underlying the salicylate-induced recovery of the plasma membrane expression of prestin mutants.

Acknowledgements

This work was supported by Grant-in-Aid for Scientific Research on Priority Areas 15086202 from the Ministry of Education, Culture, Sports, Science and Technology of Japan, by Grant-in-Aid for Scientific Research (B) 18390455 from the Japan Society for the Promotion of Science, by Grant-in-Aid for Exploratory Research 18659495 from the Ministry of Education, Culture, Sports, Science and Technology of Japan, by a grant from the Human Frontier Science Program, by a Health and Labour Science Research Grant from the Ministry of Health, Labour and Welfare of Japan, and by Tohoku University Global COE Program "Global Nano-Biomedical Engineering Education and Research Network Centre" to H.W., and by a Grant-in-Aid for JSPS Fellows from the Japan Society for the Promotion of Science to S.K.

References

[1] Zheng, J., Shen, W., He, D.Z.Z., Long, K.B., Madison, L.D. and Dallos, P. (2000) Prestin is the motor protein of cochlear outer hair cells. Nature 405, 149–155.
[2] Ashmore, J. (2008) Cochlear outer hair cell. Physiol. Rev. 88, 173–210.
[3] Loo, T.W. and Clarke, D.M. (1997) Correction of defective protein kinesis of human P-glycoprotein mutants by substrates and modulators. J. Biol. Chem. 272 (2), 709–712.
[4] Loo, T.W., Bartlett, M.C. and Clarke, D.M. (2005) Rescue of folding defects in ABC transporters using pharmacological chaperones. J. Bioenerg. Biomembr. 37 (6), 501–507.
[5] Janovick, J.A., Maya Nunez, G. and Conn, P.M. (2002) Rescue of hypogonadotropic hypogonadism-causing and manufactured GnRH receptor mutants by a specific protein-folding template: misrouted proteins as a novel disease etiology and therapeutic target. J. Clin. Endocrinol. Metab. 87 (7), 3255–3262.
[6] Morello, J.P., Salahpour, A., Laperriere, A., Bernier, V., Arthus, M.F., Lonergan, M., Petaja Repo, U., Angers, S., Morin, D., Bichet, D.G. and Bouvier, M. (2000) Pharmacological chaperones rescue cell-surface expression and function of misfolded V2 vasopressin receptor mutants. J. Clin. Invest. 105 (7), 887–895.
[7] Ulloa-Aguirre, A., Janovick, J.A., Brothers, S.P. and Conn, P.M. (2004) Pharmacologic rescue of conformationally-defective proteins: implications for the treatment of human disease. Traffic 5 (11), 821–837.
[8] Tunstall, M.J., Gale, J.E. and Ashmore, J.F. (1995) Action of salicylate on membrane capacitance of outer hair cells from the guinea-pig cochlea. J. Physiol. 485, 739–752.
[9] Kakehata, S. and Santos-Sacchi, J. (1996) Effects of salicylate and lanthanides on outer hair cell motility and associated gating charge. J. Neurosci. 16 (16), 4881–4889.
[10] Kumano, S., Iida, K., Murakoshi, M., Naito, N., Tsumoto, K., Ikeda, K., Kumagai, I., Kobayashi, T. and Wada, H. (2005) Effects of mutation in the conserved GTSRH sequence of the motor protein prestin on its characteristics. JSME Int. J. 48C, 403–410.
[11] Kumano, S., Tan, X., He, D.Z.Z., Iida, K., Murakoshi, M. and Wada, H. (2009) Mutation-induced reinforcement of prestin-expressing cells. Biochem. Biophys. Res. Commun. 389, 569–574.
[12] Naoghare, P.K., Kwon, H.T. and Song, J.M. (2007) An automated method for in vitro anticancer drug efficacy monitoring based on cell viability measurement using a portable photodiode array chip. Lab Chip 7, 1202–1205.
[13] Iida, K., Tsumoto, K., Ikeda, K., Kumagai, I., Kobayashi, T. and Wada, H. (2005) Construction of an expression system for the motor protein prestin in Chinese hamster ovary cells. Hear. Res. 205 (1–2), 262–270.
[14] Santos Sacchi, J. (1991) Reversible inhibition of voltage-dependent outer hair cell motility and capacitance. J. Neurosci. 11, 3096–3110.
[15] Oliver, D., He, D.Z.Z., Klöcker, N., Ludwig, J., Schulte, U., Waldegger, S., Ruppersberg, J.P., Dallos, P. and Fakler, B. (2001) Intracellular anions as the voltage sensor of prestin, the outer hair cell motor protein. Science 292 (5525), 2340–2343.

FEBS Letters 584 (2010) 2872–2876

journal homepage: www.FEBSLetters.org

Atomic force microscopy imaging of the structure of the motor protein prestin reconstituted into an artificial lipid bilayer

Shun Kumano, Michio Murakoshi, Koji Iida, Hiroshi Hamana, Hiroshi Wada *

Department of Bioengineering and Robotics, Tohoku University, 6-6-01 Aoba-yama, Sendai 980-8579, Japan

ARTICLE INFO

Article history:
Received 2 March 2010
Revised 29 April 2010
Accepted 30 April 2010
Available online 7 May 2010

Edited by Sandro Sonnino

Keywords:
Prestin
Membrane protein
Atomic force microscopy
Outer hair cell
Inner ear

ABSTRACT

Prestin is the motor protein of cochlear outer hair cells and is essential for mammalian hearing. The present study aimed to clarify the structure of prestin by atomic force microscopy (AFM). Prestin was purified from Chinese hamster ovary cells which had been modified to stably express prestin, and then reconstituted into an artificial lipid bilayer. Immunofluorescence staining with anti-prestin antibody showed that the cytoplasmic side of prestin was possibly face up in the reconstituted lipid bilayer. AFM observation indicated that the cytoplasmic surface of prestin was ring-like with a diameter of about 11 nm.

1. Introduction

The basis of electromotility of outer hair cells (OHCs) which realizes the high sensitivity of mammalian hearing is considered to be the motor protein prestin [1]. Several characteristics of prestin have been gradually clarified [2]. Murakoshi et al. [3] detected prestin in the plasma membrane of prestin-transfected Chinese hamster ovary (CHO) cells using Qdots as topographic markers and observed ring-like structures, possibly prestin, by atomic force microscopy (AFM). Mio et al. [4] observed prestin purified from prestin-transfected insect cells by transmission electron microscopy (TEM) and found prestin to be a bullet-shaped molecule. Although those two studies are significant, their observed images differed, indicating that the structure of prestin was unclear. Thus, the aim of the present study was to clarify such structure by reconstitution of purified prestin into an artificial lipid bilayer and observation of the prestin-reconstituted lipid bilayer by AFM.

2. Materials and methods

2.1. Purification of prestin

The purification of prestin was performed by the method established in our previous study with some modifications [5]. CHO cells which had been modified to stably express C-terminal 3×FLAG-tagged prestin were suspended in Tris–KCl buffer (10 mM Tris, 150 mM KCl, pH 7.4) and sonicated, followed by centrifugation at 1000×*g* for 7 min at 4 °C to remove nuclei and undisrupted cells. The obtained supernatant was centrifuged at 20360×*g* at 4 °C for 2 h to collect the membrane fraction of the cells. Membrane proteins were solubilized by resuspending the obtained membrane fraction in Tris–KCl buffer containing 10 mM *n*-nonyl-β-D-thiomaltopyranoside (NTM, Dojindo, Kumamoto, Japan). After 3-h incubation on ice, samples were centrifuged at 20360×*g* at 4 °C for 3 h to remove non-solubilized proteins. The supernatant was applied to a column filled with anti-FLAG affinity gel (Sigma–Aldrich, St. Louis, MO). The column was then washed with Tris–KCl buffer containing 0.065 mM Fos-Cholin-16 (Anatrace, Maumee, OH) to replace the detergent NTM with Fos-Choline-16. Afterward, prestin was competitively eluted with 1 ml of that buffer containing 500 μg/ml of 3×FLAG peptide (Sigma–Aldrich). Whether prestin was purified or not was confirmed by SDS–PAGE, followed by Western blotting with anti-FLAG antibody and HRP-conjugated anti-mouse IgG antibody and by silver staining.

Abbreviations: OHC, outer hair cell; CHO, Chinese hamster ovary; AFM, atomic force microscopy; TEM, transmission electron microscopy

* Corresponding author. Hiroshi Wada, Department of Bioengineering and Robotics, Tohoku University, 6-6-01 Aoba-yama, Sendai 980-8579, Japan. Fax: +81 22 795 6939.
E-mail address: wada@cc.mech.tohoku.ac.jp (H. Wada).

0014-5793/$36.00
doi:10.1016/j.febslet.2010.04.076

2.2. Reconstitution of prestin into a preformed lipid bilayer

The method of direct reconstitution of membrane proteins into a preformed lipid bilayer was applied in the present study [6]. An artificial lipid bilayer was formed on mica using dioeoyl-phosphatidylcholine (DOPC) and dipalmitoyl-phosphatidylcholine (DPPC) (Avanti Polar Lipids, Alabaster, AL). The lipid bilayer was preincubated for 30 min at 4 °C with Tris–KCl buffer containing 5 mM $CaCl_2$ and 0.0065 mM Fos-cholin-16 for equilibration of the detergent within the lipid bilayer. Afterward, such bilayer was incubated with Tris–KCl buffer containing purified prestin, 5 mM $CaCl_2$ and 0.039 mM Fos-cholin-16 for 15 min at 4 °C. Excess prestin was then removed by extensive rinsing with Tris–KCl buffer. As a negative control, the lipid bilayer treated with detergent but without prestin was also prepared.

2.3. Staining of prestin in the reconstituted lipid bilayer

The existence of prestin in the lipid bilayer was confirmed by immunofluorescence staining. The prestin-reconstituted lipid bilayer was incubated with Block Ace (Dainippon Pharmaceutical Co. Osaka, Japan) for 30 min at 37 °C to avoid non-specific binding of antibodies. Afterward, that bilayer was stained with goat anti-prestin N-terminus primary antibody (Santa Cruz Biotechnology, Santa Cruz, CA, USA) at a dilution of 1:100 in PBS overnight at 4 °C and with anti-goat IgG Texas Red (Santa Cruz Biotechnology) at a dilution of 1:200 in PBS at 37 °C for 60 min. The stained lipid bilayer was observed by confocal microscopy.

2.4. AFM imaging

The height images of the lipid bilayer were acquired in Tris–KCl buffer filtered with a 0.2-μm nylon filter by Multimode V AFM with a Nanoscope V controller (Veeco, Santa Barbara, CA) at 24–26 °C. V-shaped Si_3N_4 cantilevers (OMCL-TR400PSA-2, Olympus, Tokyo, Japan) with a spring constant of 0.06 N/m were used. The AFM was operated in the oscillation imaging mode (Tapping mode™, Digital Instruments) at a scan frequency of 1–0.5 kHz. In the present study, three types of images were obtained by AFM, namely, low- (5.0 × 5.0 μm), middle- (1.0 × 1.0 μm) and high-magnification images (300 × 300 nm). Each scan line has 256 and 512 points of data and an image consists of 256 and 512 scan lines for low magnification images and for middle- and high-magnification images, respectively. Obtained AFM images were flattened by use of a software program (NanoScope v7.00, Veeco) to eliminate background slopes and to correct dispersions of individual scanning lines. In addition, only high-magnification images were low-pass filtered to reduce high frequency noise. When the observed structure was ring-like, the distance between two peaks based on the cross sections was taken to be its diameter, as was done in our previous study [3].

3. Results

3.1. Purification of prestin

Whether prestin was indeed purified or not was investigated by SDS–PAGE, followed by Western blotting and silver staining. Results of Western blotting and silver staining are shown in Fig. 1A and B, respectively. In the Western blotting image, the 100 kDa band, probably showing prestin, was detected. In the results of silver staining, only one band corresponding to the band observed in Western blotting was recognized.

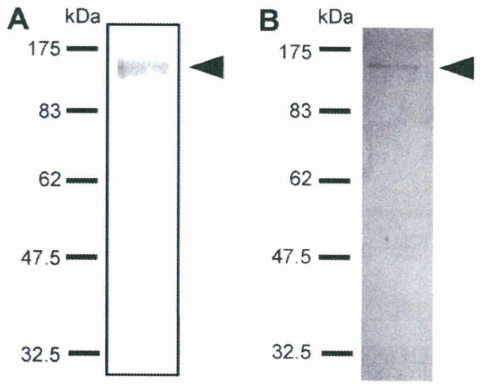

Fig. 1. Results of Western blotting and silver staining. (A) Western blotting data. A 100 kDa band probably showing prestin is seen. (B) Result of silver staining of SDS–PAGE gel. Only one band at 100 kDa, which was thought to correspond to the band detected in the result of Western blotting, is recognized.

3.2. Immunofluorescence staining of the prestin-reconstituted lipid bilayer

After the reconstitution process, immunofluorescence staining was employed to investigate whether prestin had been incorporated into the preformed lipid bilayer. Representative immunofluorescence images of the prestin-reconstituted lipid bilayer and negative control sample are shown in Fig. 2. Red fluorescence was detected in the prestin-reconstituted lipid bilayer but not in the negative control sample.

3.3. AFM imaging of the lipid bilayer

The AFM height image of the lipid bilayer without treatment showed two kinds of flat domains (Fig. 3A). A similar image was also obtained from the negative control sample (Fig. 3B). Unlike those two images, in addition to the flat domain, bumpy domains indicated by white arrows were detected in the low magnification AFM image of the prestin-reconstituted lipid bilayer (Fig. 3C). The boxed area in Fig. 3C was scanned by AFM and the obtained image is depicted in Fig. 3D. Dense small particles, some of which were recognized as ring-like structures, can be observed in that image. To clearly visualize the observed particles, the boxed area in Fig. 3D was scanned by AFM, the acquired image being shown in Fig. 3E. Moreover, three-dimensional representation of Fig. 3E is depicted in Fig. 4. Many ring-like structures were confirmed to be densely embedded in the lipid bilayer. The average diameter of such structures in Fig. 3E and other AFM images which are not shown here is 11.0 ± 1.3 nm ($n = 42$).

4. Discussion

4.1. Reconstitution of prestin into an artificial lipid bilayer

After the purification process, only the 100 kDa band corresponding to the band in Western blotting data was detected by silver staining of SDS–PAGE gel, indicating that prestin had been purified. The 100 kDa band probably shows the monomer of prestin. As SDS possibly affects the binding between prestin molecules, to clearly confirm the oligomerization of purified prestin, a mild detergent such as perfluoro-octanoic acid should be used as in the study by Zheng et al. [7]. The AFM height image of the lipid bilayer without treatment shows two types of flat domains (Fig. 3A), as seen in previous studies [6,8–11]. At 24–26 °C, DOPC forms fluid-phase domains, while DPPC forms gel-phase domains. The thickness of DPPC in the gel-phase is larger than that of DOPC in

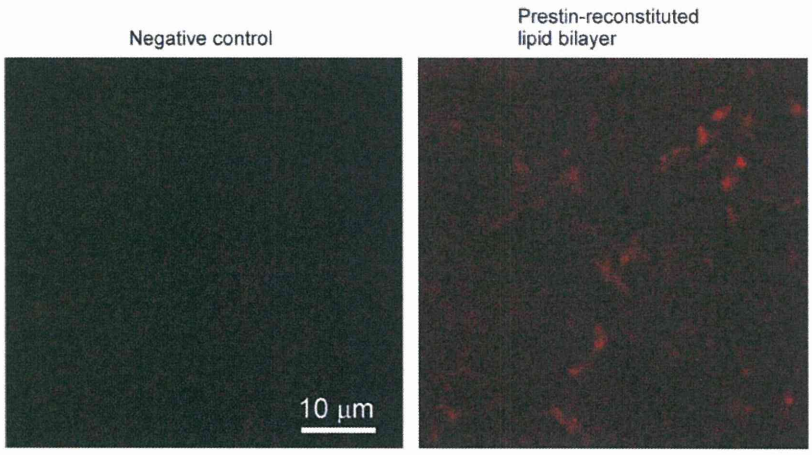

Fig. 2. Immunofluorescence staining of prestin-reconstituted lipid bilayer. Negative control sample and the prestin-reconstituted lipid bilayer were stained with anti-prestin antibody and anti-goat IgG Texas Red. Red fluorescence indicating the existence of prestin is only found in the prestin-reconstituted lipid bilayer.

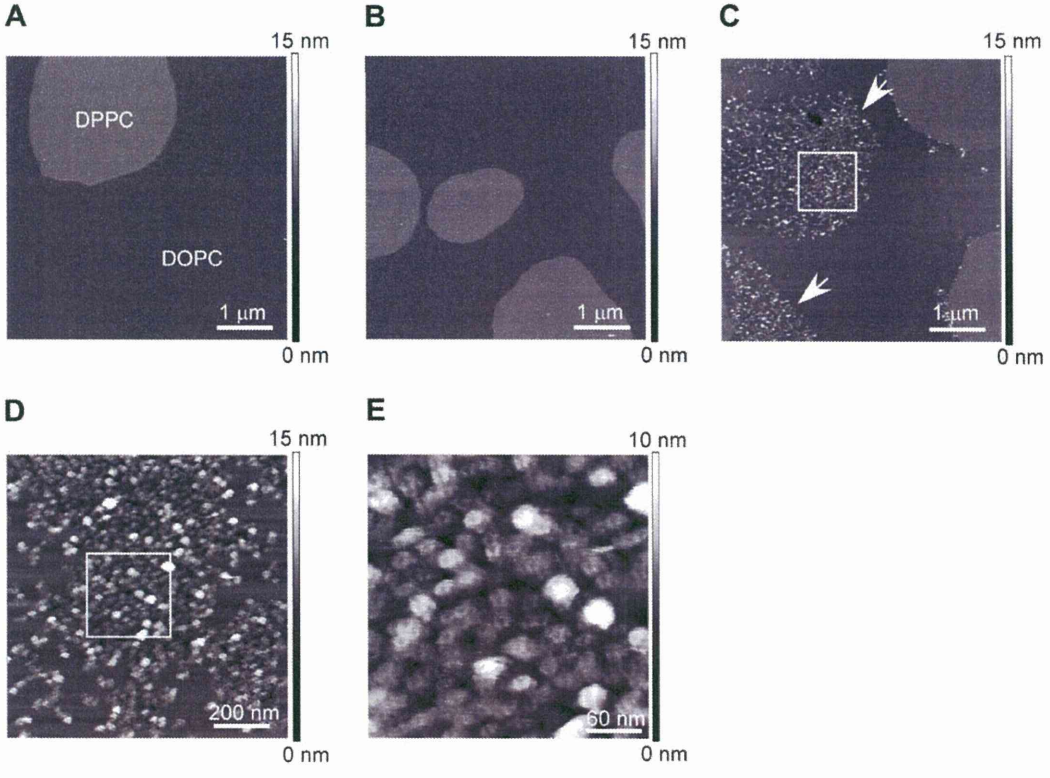

Fig. 3. AFM height images of the lipid bilayer. (A) AFM image of the lipid bilayer without treatment at low magnification. (B) AFM image of the negative control sample at low magnification. (C) AFM image of prestin-reconstituted lipid bilayer at low magnification. (D) Middle-magnification image obtained by scanning of the boxed area shown in (C). (E) High-magnification image obtained by scanning of the boxed area shown in (D). Two kinds of flat domains in (A) and (B) probably represent the domain of DPPC in the gel-phase and that of DOPC in the fluid-phase. Bumpy domains indicated by white arrows can be detected in the prestin-reconstituted lipid bilayer shown in (C). Many small particles can be found in the middle-magnification AFM images and those particles were recognized as ring-like in the high-magnification image. Such ring-like structures probably show prestin molecules.

the fluid-phase, thus indicating that the two types of observed domains were due to the difference in the thickness between the two lipids. After the reconstitution process, immunofluorescence staining using anti-prestin antibody showed that prestin existed in the reconstituted lipid bilayer (Fig. 2). In the AFM image, the bumpy domains, which probably corresponded to prestin, were recognized only in DOPC domains of the prestin-reconstituted lipid bilayer. Milhiet et al. [6] have also suggested that proteins of interest were reconstituted only into the DOPC domains in the fluid state. Thus, the present study and their study imply that proteins tend to be reconstituted into the DOPC domains in the fluid state. In the AFM image at high-magnification, ring-like structures probably showing prestin were densely reconstituted into the lipid bilayer. However, the alignment of such structures as found in the OHC plasma membrane by Sinha et al. [12] was not detected, which might have resulted from differences in the environment

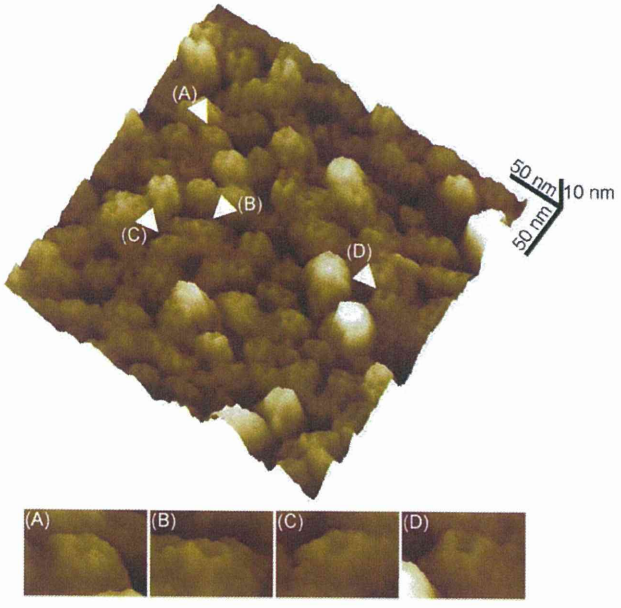

Fig. 4. Three-dimensional AFM height image of the prestin-reconstituted lipid bilayer. This figure was created from Fig. 3E. Representative examples of ring-like structures were digitally magnified and are shown (A and B). Ring-like structures, considered to be similar to those observed in the study of Murakoshi et al. [3], are found to be densely embedded in the lipid bilayer.

Table 1
Comparison of the size of prestin.

Sample	Method	Diameter (nm)	References
OHC plasma membrane	AFM	11–25	Le Grimellec et al. [15]
Purified prestin	TEM	7.7–9.6	Mio et al. [4]
Prestin-expressing CHO cell plasma membrane	AFM	9.6/13.0	Murakoshi et al. [3]
OHC plasma membrane	AFM	10	Sinha et al. [12]
Prestin-reconstituted lipid bilayer	AFM	11.0 ± 1.3	This study

between the OHC plasma membrane and the artificial lipid bilayer. The existence of actin cytoskeleton in OHCs and that of mica in the present study would affect the alignment of prestin.

4.2. Orientation of prestin

The orientation of prestin should be considered to confirm which side of prestin was observed by AFM, the extracellular side or the cytoplasmic side. Previous reports have suggested that when membrane proteins were reconstituted into a preformed lipid bilayer as done in the present study, their unidirectional orientation was obtained [6,13,14], indicating that all prestin molecules reconstituted into the lipid bilayer might be oriented in the same direction. In the present study, the standard deviation of the diameter of the observed ring-like structure, 1.3 nm, was small. Small standard deviation might increase the possibility that only either prestin molecules whose extracellular side was exposed or such molecules whose cytoplasmic side was exposed existed in the reconstituted lipid bilayer. Data showed in the previous reports, small standard deviation of the diameter and successful staining of such bilayer with anti-prestin antibody which binds to the cytoplasmic side of prestin possibly implied that the cytoplasmic side of prestin was face up. Although the possibility that the extracellular side of a few prestin molecules was exposed was not completely ruled out, it was considered that AFM possibly visualized the cytoplasmic side of prestin in the present study.

4.3. Structure and size of prestin

The AFM image of the prestin-reconstituted lipid bilayer showed dense ring-like structures, each with a diameter of 11.0 ± 1.3 nm, which were probably the surface structure of the cytoplasmic side of prestin. The previously reported sizes of prestin obtained by observation of the cytoplasmic side of prestin are listed in Table 1 [3,4,12,15]. Although it is unclear whether the particles detected in OHC plasma membranes are only comprised of prestin or not, our result is consistent with the previously reported sizes, supporting the assumption that the observed structures were prestin.

Le Grimellec et al. [15] found structures with a central depression in the cytoplasmic side of the OHC plasma membrane by AFM. Murakoshi et al. [3] showed by AFM that prestin might form a ring-like structure. On the other hand, Mio et al. [4] suggested that prestin is a bullet-shaped molecule which protrudes into the cytoplasmic side. Although Sinha et al. [12] found 10-nm particles in the cytoplasmic side of the OHC plasma membrane by AFM, whether those particles were ring-like or not was not specified. Thus, the structure of prestin has been a controversial issue. Our results demonstrate that prestin may form a ring-like structure with a diameter of about 11 nm, which agrees with results of Le Grimellec et al. [15] and Murakoshi et al. [3].

In summary, the present study attempted to visualize prestin purified and reconstituted into the artificial lipid bilayer by AFM. From the obtained AFM image, the cytoplasmic surface of prestin was indicated to be ring-like with a diameter of about 11 nm.

Acknowledgements

This work was supported by Grant-in-Aid for Scientific Research on Priority Areas 15086202 from the Ministry of Education, Culture, Sports, Science and Technology of Japan, by Grant-in-Aid for Scientific Research (B) 18390455 from the Japan Society for the Promotion of Science, by Grant-in-Aid for Exploratory Research 18659495 from the Ministry of Education, Culture, Sports, Science and Technology of Japan, by a grant from the Human Frontier Science Program, by a Health and Labour Science Research Grant from the Ministry of Health, Labour and Welfare of Japan, and by Tohoku University Global COE Program "Global Nano-Biomedical Engineering Education and Research Network Centre" to H.W., and by a Grant-in-Aid for JSPS Fellows from the Japan Society for the Promotion of Science to S.K.

References

[1] Zheng, J., Shen, W., He, D.Z.Z., Long, K.B., Madison, L.D. and Dallos, P. (2000) Prestin is the motor protein of cochlear outer hair cells. Nature 405, 149–155.
[2] Ashmore, J. (2008) Cochlear outer hair cell. Physiol. Rev. 88, 173–210.
[3] Murakoshi, M., Iida, K., Kumano, S. and Wada, H. (2009) Immune atomic force microscopy of prestin-transfected CHO cells using quantum dots. Pflugers Arch. 457, 885–898.
[4] Mio, K., Kubo, Y., Ogura, T., Yamamoto, T., Arisaka, F. and Sato, C. (2008) The motor protein prestin is a bullet-shaped molecule with inner cavities. J. Biol. Chem. 283, 1137–1145.
[5] Iida, K., Murakoshi, M., Kumano, S., Tsumoto, K., Ikeda, K., Kobayashi, T., Kumagai, I. and Wada, H. (2008) Purification of the motor protein prestin from Chinese hamster ovary cells stably expressing prestin. JBSE 3, 221–234.
[6] Milhiet, P.E., Gubellini, F., Berquand, A., Dosset, P., Rigaud, J.L., Le Grimellec, C. and Levy, D. (2006) High-resolution AFM of membrane proteins directly incorporated at high density in planar lipid bilayer. Biophys. J. 91, 3268–3275.
[7] Zheng, J., Du, G.G., Anderson, C.T., Keller, J.P., Orem, A., Dallos, P. and Cheatham, M. (2006) Analysis of the oligomeric structure of the motorprotein prestin. J. Biol. Chem. 281, 19916–19924.
[8] Morandat, S. and Kirat, K.E. (2006) Membrane resistance to Triton X-100 explored by real-time atomic force microscopy. Langmuir 22, 5786–5791.

[9] Berquand, A., Levy, D., Gubellini, F., Le Grimellec, C. and Milhiet, P. (2007) Influence of calcium on direct incorporation of membrane proteins into in-plane lipid bilayer. Ultramicroscopy 107, 928–933.
[10] Francius, G., Dufour, S., Deleu, M., Paquot, M., Mingeot-Leclercq, M. and Dufrêne, Y.E. (2008) Nanoscale membrane activity of surfactins: influence of geometry, charge and hydrophobicity. Biochim. Biophys. Acta 1778, 2058–2068.
[11] Mingeot-Leclercq, M., Deleu, M., Brasseur, R. and Dufrêne, Y.F. (2008) Atomic force microscopy of supported lipid bilayers. Nat. Protoc. 3, 1654–1659.
[12] Sinha, G.P., Sabri, F., Dimitriadis, E.K. and Iwasa, K.H. (2010) Organization of membrane motor in outer hair cells: an atomic force microscopic study. Pflugers Arch. 459, 427–439.
[13] Rigaud, J., Paternostre, M. and Bluzat, A. (1988) Mechanism of membrane protein insertion into liposomes during reconstitution procedures involving the use of detergents. 2. Incorporation of the light-driven proton pump bacteriorhodopsin. Biochemistry 27, 2677–2688.
[14] Rigaud, J., Pitard, B. and Levy, D. (1995) Reconstitution of membrane proteins into liposome: application to energy-transducing membrane proteins. Biochim. Biophys. Acta 1231, 223–246.
[15] Le Grimellec, C., Giocondi, M.C., Lenoir, M., Vater, M., Sposito, G. and Pujol, R. (2002) High-resolution three-dimensional imaging of the lateral plasma membrane of cochlear outer hair cells by atomic force microscopy. J. Comp. Neurol. 451, 62–69.

CLINICAL GENETICS
An International Journal of Genetics, Molecular, and Personalized Medicine

Clin Genet 2010: 78: 464–470
Printed in Singapore. All rights reserved

CLINICAL GENETICS
doi: 10.1111/j.1399-0004.2010.01407.x

Short Report

A large cohort study of *GJB2* mutations in Japanese hearing loss patients

Tsukada K, Nishio S, Usami S, and the Deafness Gene Study Consortium. A large cohort study of *GJB2* mutations in Japanese hearing loss patients. Clin Genet 2010: 78: 464–470. © John Wiley & Sons A/S, 2010

GJB2 is the gene most frequently associated with hereditary hearing loss, and the *GJB2* mutation spectrums vary among different ethnic groups. In this study, the mutation spectrum as well as clinical features of patients with *GJB2* mutations as found in more than 1000 Japanese hearing loss families are summarized. The present results show that the frequency of *GJB2* mutations in the Japanese population with hearing loss is 14.2% overall and 25.2% in patients with congenital hearing loss. c.235*del*C was the most frequent allele (49.8%), was associated with a more severe phenotype, and was mainly found in patients who were diagnosed by the age of 3. In contrast, the second most frequent was p.V37I (16.5%), which has a milder phenotype and was mainly found in patients diagnosed at a higher age. Additional clinical features in hearing loss patients with *GJB2* mutations in this study were the near absence of tinnitus, vestibular dysfunction and inner ear malformations.

K Tsukada, S Nishio, S Usami and the Deafness Gene Study Consortium

Department of Otorhinolaryngology, Shinshu University School of Medicine, 3-1-1 Asahi, Matsumoto 390-8621, Japan

Key words: clinical features – genotype – phenotype correlations – *GJB2* – hearing loss – mutation

Corresponding author: Shin-ichi Usami, MD, PhD, Department of Otorhinolaryngology, Shinshu University School of Medicine, 3-1-1 Asahi, Matsumoto 390-8621, Japan.
Tel.: +81 263 37 2666;
fax: +81 263 36 9164;
e-mail: usami@shinshu-u.ac.jp

Received 27 November 2009, revised and accepted for publication 15 February 2010

Mutations in the *GJB2* gene have recently been of particular interest because *GJB2* is the commonest causative gene for hereditary hearing loss in all populations. To date, more than 100 variations have been reported worldwide (see the Connexin-deafness homepage: http://www.davinc.crg.es/deafness) and the mutation spectrums vary among different ethnic groups. There have been many papers describing the frequency of *GJB2* mutations among hearing loss populations, but most studies have been based on small numbers of patients from a single center. A large cohort study may prevent bias and provide a more precise estimate of mutation frequencies. Therefore, with the goal of establishing a database of the mutations found in the East Asian populations, we estimated the *GJB2* mutation frequency and spectrum as well as associated clinical features using more than 1500 Japanese hearing loss families collected from multiple centers.

Subjects and methods

Subjects

Data on 3056 Japanese subjects of 1511 independent families were collected from 33 ENT departments nationwide in Japan. All subjects gave prior informed consent for participation in the project, which was approved by the ethical committee of each hospital. Of the 1511 probands, 1343 had bilateral sensorineural hearing loss and 168 had unilateral sensorineural hearing loss. The control group consisted of 252 unrelated Japanese individuals without any noticeable hearing loss evaluated by auditory testing.

Mutation analysis

To identify *GJB2* mutations, a DNA fragment containing the entire coding region was sequenced as described elsewhere (1). Screening for the known

large DFNB1 deletions was performed in the patients with a single heterozygous allele without the presence of a second pathogenic mutant allele, but none were detected (data not shown).

Computational analysis

To evaluate the importance of each amino acid affected by novel missense mutations found in this study, we used a computational analysis program for identification of functionally and structurally important residues in protein sequences: CONSEQ (http://conseq.tau.ac.il/index.html).

Clinical evaluations

Hearing levels were determined by pure-tone audiometry. For the young patients, conditioned orientation response audiometry (COR) or auditory steady-state response (ASSR) were used. Clinical data, including hearing loss progression, episodes of tinnitus and vestibular dysfunction (vertigo, dizziness, faintness), were collected by anamnestic evaluation. Thin section temporal bone computed tomography (CT) was used to investigate inner ear malformations.

Results

GJB2 mutation spectrum in hearing loss probands

There were a total of 26 *GJB2* variants observed in the ascertained probands with bilateral hearing loss (Table 1). Fourteen of those were missense mutations. To evaluate the evolutionary conservation of the amino acids affected by these missense mutations, we used a computational alignment program CONSEQ (not shown). On the basis of this alignment program, all missense mutations had changed evolutionary conserved amino acids, except for p.T123N and p.Y68C. Because p.N54S and p.M195V were found in the compound heterozygous state, they are likely to be pathogenic. Eight of the mutations were found in the control group (Table 1). p.V27I, p.E114G, p.I203T (1, 2), and p.T123N (3), frequently found in both probands and controls, were thought to be non-pathological polymorphisms. The c.235*del*C and p.V37I mutations found in the control group most likely represent the detection of carriers.

Frequency of *GJB2* mutations in hearing loss probands

With regard to the frequency of *GJB2* mutations in the 1343 independently ascertained probands with bilateral hearing loss, 191 (14.2%) had at least one pathogenic *GJB2* mutant allele (Table 2). The most prevalent mutation was c.235*del*C (49.8% of all pathogenic mutant alleles) and the second most frequent was p.V37I (16.5%) (Fig. 1).

The frequency of *GJB2* mutations was significantly higher in probands who were diagnosed at an earlier age: 25.7% (108/420) in those diagnosed at age 0–3, 14.9% (15/101) in those diagnosed at age 4–5, and 7.8% (49/627) in age 6 or over (Table 2). c.235*del*C was also significantly higher in probands diagnosed at an earlier age (58.5%) compared to those who were diagnosed at the age of 6 and over (19.6%) ($p < 0.001$; χ^2 test). In contrast, p.V37I was significantly more frequent in probands who were diagnosed at the ages of 4–5 (36.4%) or 6 and over (41.1%) than in prelingual hearing loss probands (6.9%) ($p < 0.001$; χ^2 test) (Fig. 1).

Audiologic studies

Of the total 3056 subjects, 134 with bilateral hearing loss and biallelic *GJB2* mutations were selected for audiologic studies. We excluded 22 subjects who were from a family with another subject who had the same mutation. In the remaining 112 subjects, audiometric results were available for 105 probands, of 23 different genotypes. Figure 2 shows a collection of overlapping audiograms from those 105 subjects. We compared the hearing levels in the six genotypes that were shared by five or more subjects. The subjects with the p.V37I allele had significantly milder hearing loss ($p < 0.027$; Mann–Whitney *U* test).

p.V37I/p.R143W showed a significantly worse hearing level than p.V37I/p.V37I ($p = 0.025$; Mann–Whitney *U* test) and also tended to be worse than p.V37I/c.235*del*C ($p = 0.076$; Mann–Whitney *U* test). Moreover, comparison of c.235*del*C/c.235*del*C ($n = 35$) and c.235*del*C/p.R143W ($n = 13$) revealed that subjects with the p.R143W allele had a significantly worse hearing level than homozygotes ($p = 0.025$; Mann–Whitney *U* test).

Twenty-six subjects with biallelic *GJB2* mutations were followed at least two years by audiometric testing with progression of hearing loss seen in four subjects (15%), two (7%) of those being unilateral progression and two (7%) being bilateral progression.

Clinical findings

Based on the data availability, clinical findings were statistically evaluated. Episodes of tinnitus in patients with *GJB2* mutations were at a

Table 1. *GJB2* variants in deafness patients and controls

		Patients					Controls					
Amino acid change	Nucleotide change	Allele (n = 2686)	Allele frequency (%)	Homozygous (n)	Compound heterozygous (n)	Heterozygous (n)	Alleles (n = 504)	Allele frequency (%)	Controls (n = 252)	Carrier rate (%)	Evolutionary conservation	Reference
—	c.235 *del*C	142	5.29	34	45	28	2	0.40	2	0.80	NA	Fuse et al. (19)
p.V37I	c.109G>A	47	1.75	3	11	30	3	0.60	3	1.20	Yes	Abe et al. (1)
p.G45E[c]	c.134G>A											
p.Y136X[c]	c.408C>A	34	1.27	1	22	10					Yes	Fuse et al. (19)
p.R143W	c.427C>T	18	0.67	0	16	2					Yes	Brobby et al. (20)
—	c.176_191 *del*16bp	15	0.56	0	10	5					NA	Abe et al. (1)
—	c.299-300 *del*AT	11	0.41	0	8	3					NA	Abe et al. (1)
p.T86R	c.257C>A	8	0.30	0	5	3					Yes	Ohtsuka et al. (2)
—	c.512*ins*AACG	3	0.11	0	3	0					NA	Hismi et al. (21)
—	c.35*ins*G	2	0.07	0	2	0					NA	Estivill et al. (22)
p.I71T[b]	c.212T>C	2	0.07	0	0	2					Yes	Ohtsuka et al. (2)
p.T8M	c.23C>T	1	0.04	0	0	1					Yes	Kenna et al. (23)
p. I33N[b]	c.98T>A	1	0.04	0	0	1					Yes	This study
p.A49V[b]	c.146C>T	1	0.04	0	0	1					Yes	Ohtsuka et al. (2)
p.N54S	c.161A>G	1	0.04	0	1	0					Yes	This study
p.Y68C[a]	c.203A>G	1	0.04	0	0	1					No	This study
p.M93I	c.276G>A	1	0.04	0	1	0					Yes	Wu et al. (24)
p.K112M[b]	c.335A>T	1	0.04	0	0	1					Yes	This study
—	c.376-377 *del*AA[e]	1	0.04	0	0	1					NA	This study
p.W133X	c.398G>A	1	0.04	0	1	0					NA	Primignani et al.[f]
p.K168R[b]	c.503A>G	1	0.04	0	0	1					Yes	This study
p.M195V	c.583A>G	1	0.04	0	1	0					Yes	This study
—	c.605*ins*46bp	1	0.04	0	0	1					NA	Yuge et al. (25)
p.F191L	c.571T>C	0	0	0	0	0	1	0.20	1	0.40	yes	Feng et al. (26)
p.R127H	c.380G>A	0	0	0	0	0	1	0.20	1	0.40	yes	Seeman et al.[f]
Polymorphism												
p.V27I	c.79G>A	865	32.20	—	—	—	196	38.90	158	62.70	Yes	Kelley et al. (8)
p.E114G	c.341A>G	259	9.64	—	—	—	64	12.70	62	24.60	No	Fuse et al. (19)
p.T123N[d]	c.368C>A	18	0.67	0	3	15	2	0.40	2	0.80	No	Park et al. (3)
p. I203T	c.608T>C	112	4	—	—	—	21	4.10	21	8.30	No	Abe et al. (1)

[a]Variant probably representing polymorphism because no evolutionary conservation was observed.

[b]Variants with unproven pathogenic nature.

[c]p.G45E and p.Y136X(c.134G>E) mutations are on the same parental allele.

[d]p. T123N was found with equal frequency in the probands and controls, and three out of eight subjects with compound heterozygous state did not have any hearing loss, suggesting the polymorphic nature of p.T123N.

[e]c.376-377 delAA is thought to be a pathogenic mutation, but it was present as a single heterozygous allele without the presence of a second pathogenic mutant allele, therefore it could not clearly be classified as pathogenic in this study.

[f]Ballana E, Ventayol M, Rabionet R et al. Connexins and deafness Homepage. World wide web URL: http://www.crg.es/deafness.

Table 2. The frequency of GJB2 mutations and diagnostic age

	GJB2 mutations	Homozygote	Compound heterozygote	Heterozygote
Total (n = 1343)	191 (14.2%)	38 (2.8%)	63 (4.7%)	90 (6.7%)
0–3 y.o. (n = 420)	108 (25.7%)	32 (7.6%)	47 (11.2%)	29 (6.9%)
4–5 y.o. (n = 101)	15 (14.9%)	1 (0.99%)	6 (5.9%)	8 (7.9%)
≥6 y.o. (n = 627)	49 (7.8%)	3 (0.48%)	4 (0.64%)	42 (6.7%)
Unknown (n = 195)	19	2	6	11

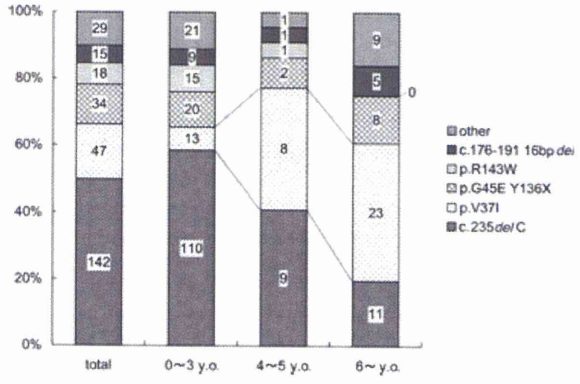

Fig. 1. Frequency of mutant GJB2 alleles in different diagnostic age groups. c.235*del*C was mainly found in the group diagnosed at up to 3 years, where it was significantly higher than in age 6 and over ($p < 0.01$; χ^2 test). On the contrary, p.V37I was mainly found in the diagnostic age groups of 4–5, and 6 and over, at a rate significantly higher than in up to age 3 ($p < 0.01$).

significantly lower rate (7/75: 9.3%) than in all bilateral hearing loss probands (520/1022: 50.9%) ($p < 0.001$; χ^2 test). Concerning episodes of vestibular dysfunction, only 4% (3/75) of those with biallelic *GJB2* mutations had vertigo, dizziness, or faintness, while 25.1% of all hearing loss probands (258/1029) had vertigo ($p < 0.001$; χ^2 test). Inner ear abnormalities were significantly lower in patients with biallelic *GJB2* mutations (5/62: 8.1%) than in all bilateral hearing loss probands (126/599: 21%) ($p = 0.014$; χ^2 test). In the five patients with biallelic *GJB2* mutations who had inner ear abnormalities, enlarged vestibular aqueduct (EVA) was found in three and the other two had hypoplasty of the cochlea and semicircular canals.

Discussion

GJB2 mutations were found in 14.2% of our bilateral hearing loss probands and 25.2% of those diagnosed at age 0–3 (for practicality categorized as congenital hearing loss). In previous studies in East Asia (1–6), frequency of *GJB2* mutations ranged from 10% to 38% in smaller cohorts. In the present large study using Japanese hearing loss patients collected from multiple centers, we could more accurately estimate the frequency of *GJB2* mutations in Japan and the mutation spectrum. We also found two novel mutation candidates, p.N54S and p.M195V, which cause non-conservative amino acid changes.

In Asian populations, c.235*del*C is the most common *GJB2* mutation, and its allele frequency in patients ranges from about 5% to 22% (1–7). The present study reconfirmed this mutation's high frequency in the Japanese hearing loss population. c.235*del*C accounted for 5.3% of the deafness alleles in all patients and 13.1% of those in patients diagnosed at age 0–3.

The p.V37I mutation was originally reported as a polymorphism (8); however, recent reports tend to consider it pathogenic with a milder phenotype (9–12) and this was supported by our results.

Only four out of twenty-six probands showed progressive hearing loss, and bilateral progression was found in only two of those, with a deterioration of less than 20 dB. Therefore, our study supports the previously reported notion that hearing loss due to *GJB2* mutations is typically non-progressive (13–15). With regard to the milder phenotype of p.V37I, none of the five patients with this mutation showed progression. We conclude that this mutation causes milder congenital hearing loss which may not be noticed until age 4 or older.

However, even though it was the second most frequent allele in the hearing loss patients, the p.V37I allele was the most frequent in the control subjects. This may be due to the milder phenotype and non-progression of patients with p.V37I mutation, who therefore either do not visit ENT clinics or do not receive a recommendation for genetic testing from clinicians. Therefore, ENT clinicians should bear in mind the existence of the milder phenotype caused by the p.V37I mutation.

We found that patients with c.235*del*C/p.R143W were significantly more severely affected than those with other c.235*del*C-containing phenotypes. A recent study also reported that the hearing level of c.35*del*G/p.R143W is significantly worse than that of homozygous c.35*del*G (9).

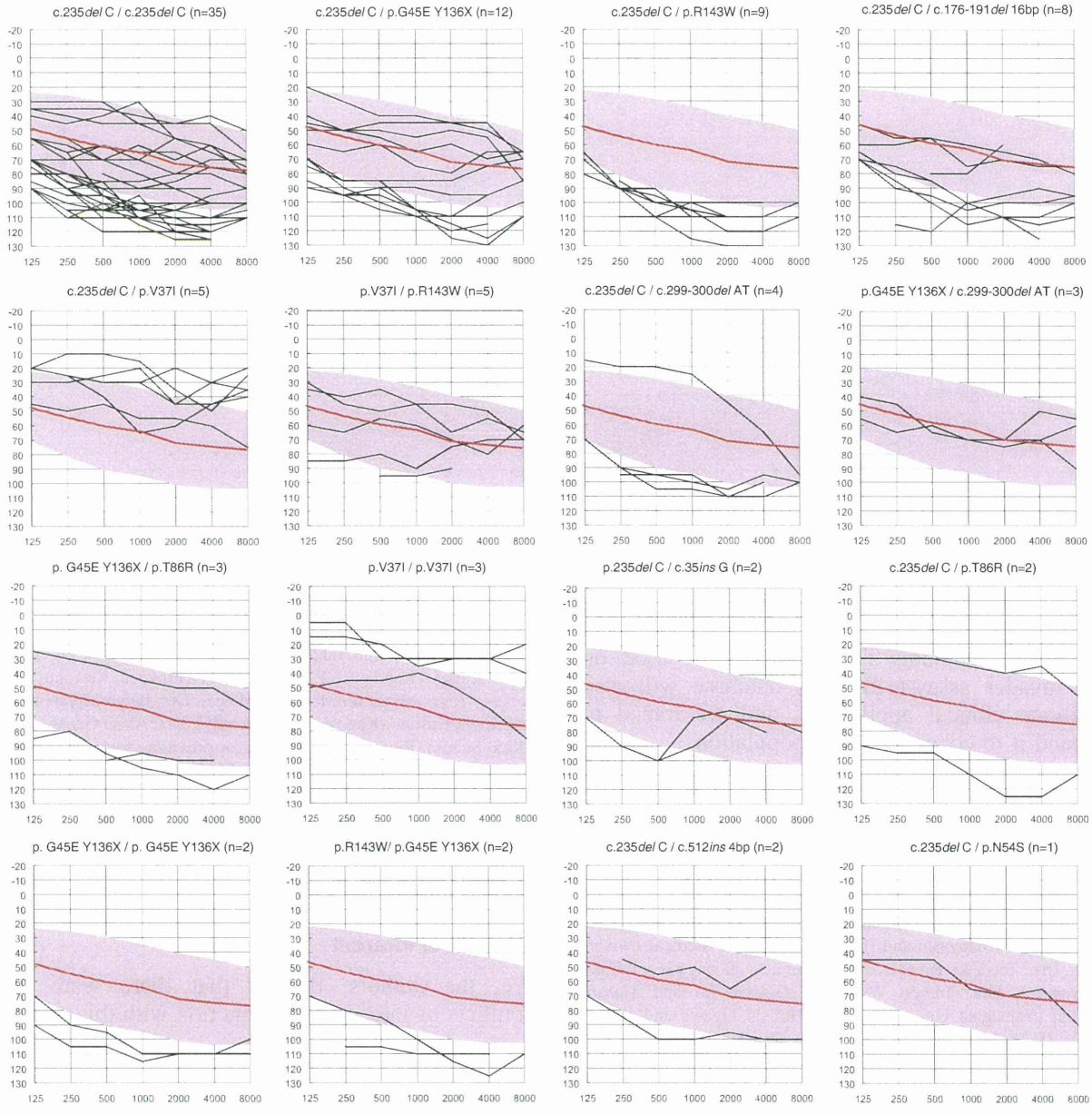

Fig. 2. Overlapping audiograms from the better ear for each genotype. The average audiogram from all subjects (1343 with bilateral sensorineural hearing loss) is indicated by a red line with standard deviation (shadow).

We compared homozygous for c.235*del*C with compound heterozygous with p.R143W (except for the p.V37I allele, which is thought to be a milder phenotype), finding the hearing level of the latter to be significantly worse. Also, comparing only the milder p.V37I allele, the hearing level of p.V37I/p.R143W was worse than that of p.V37I/p.V37I and p.V37I/c.235*del*C. These results suggest that p.R143W leads to a worse phenotype than other *GJB2* mutations.

The majority of our probands did not have tinnitus or vestibular dysfunction. Only 8% (5/65) of the patients with biallelic *GJB2* mutations had inner ear malformation, significantly lower than in the overall population with bilateral hearing loss, and in accordance with previous reports (14, 16, 17). Hearing loss patients with *GJB2* mutations also had a near absence of tinnitus, vestibular dysfunction and inner ear malformations.

In conclusion, our results describe the frequency of *GJB2* mutations and associated clinical features in a large Japanese cohort. Recently, based on our database of mutation spectrums found in Japanese, we have developed a genetic test for use in

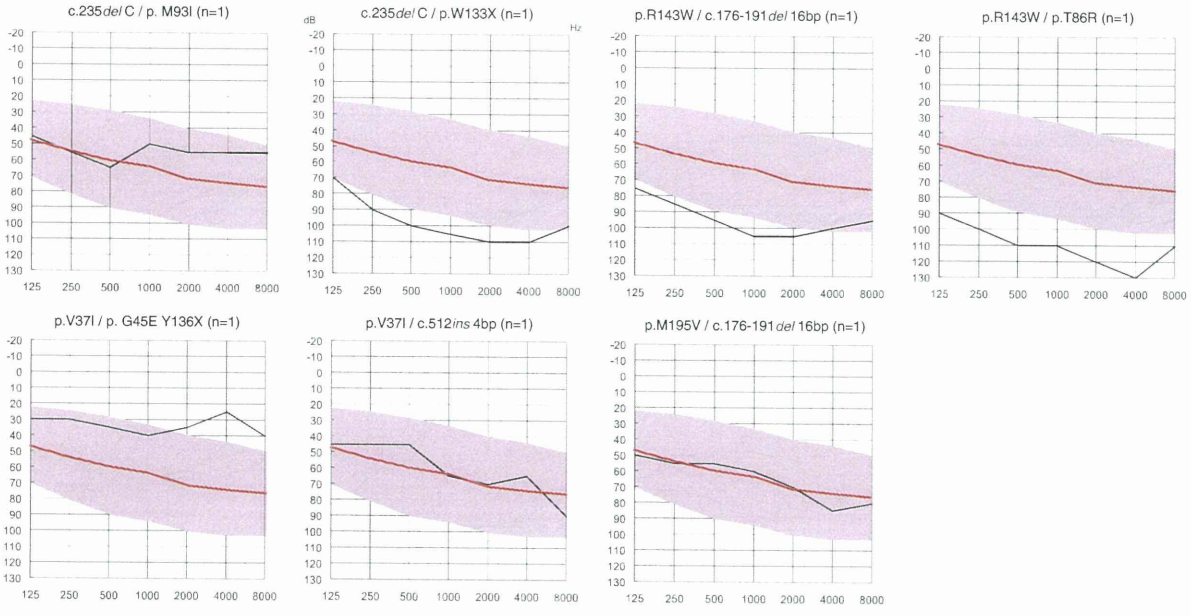

Fig. 2. Continued

diagnostic screening for hearing loss based on the invader assay (18). This database will also facilitate clinical application, and we intend to expand it to cover all Asian populations.

Acknowledgements

We thank the participants of the Deafness Gene Study Consortium: Drs. Norihito Takeichi and Satoshi Fukuda (Hokkaido University), Drs. Atsushi Namba and Hideichi Shinkawa (Hirosaki University), Drs. Yumiko Kobayashi and Hiroaki Sato (Iwate Medical University), Drs. Tetsuaki Kawase and Toshimitsu Kobayashi (Tohoku University), Drs. Tomoo Watanabe, Tsukasa Ito and Masaru Aoyagi (Yamagata University), Drs. Hiroshi Ogawa and Koichi Omori (Fukushima Medical University), Drs. Kotaro Ishikawa and Keiichi Ichimura (Jichi Medical University), Drs. Kyoko Nagai and Nobuhiko Furuya (Gunma University), Drs. Shuntaro Shigihara, Yasuyuki Nomura and Minoru Ikeda (Nihon University School), Drs. Tetsuo Ikezono and Toshiaki Yagi (Nippon Medical School), Dr. Shunichi Tomiyama (Nippon Medical School Tama Nagayama Hospital), Drs. Hiromi Kojima, Yuika Sakurai and Hiroshi Moriyama (Jikei University), Dr. Kozo Kumakawa (Toranomon Hospital), Dr. Satoko Abe (Abe ENT Clinic), Drs. Hajime Sano and Makito Okamoto (Kitasato University), Dr. Satoshi Iwasaki (Hamamatsu Medical University), Dr. Kazuhiko Takeuchi (Mie University), Dr. Masako Nakai (Shiga Medical Center for Children), Drs. Masahiko Higashikawa and Hiroshi Takenaka (Osaka Medical College), Drs. Yuko Saito, Masafumi Sakagami (Hyogo College of Medicine), Dr. Yasushi Naito (Kobe City Medical Center General Hospital), Drs. Keiji Fujihara, Akihiro Sakai and Noboru Yamanaka (Wakayama Medical University), Drs. Kunihiro Fukushima, and Kazunori Nishizaki (Okayama University), Drs. Kazuma Sugahara and Hiroshi Yamashita (Yamaguchi University), Drs. Naoto Hato and Kiyofumi Gyo (Ehime University), Drs. Yasuhiro Kakazu and Shizuo Komune (Kyushu University), Drs. Mayumi Sugamura and Takashi Nakagawa (Fukuoka University), Dr. Haruo Takahashi (Nagasaki University), Dr. Yukihiko Kanda (Kanda ENT Clinic), Drs. Hirokazu Kawano and Tetsuya Tono (Miyazaki Medical College), Drs. Ikuyo Miyanohara andYuichi Kurono (Kagoshima University), Drs. Akira Ganaha and Mikio Suzuki (Ryukyus University), for providing samples of their patients. We also thank A. C. Apple-Mathews for help in preparing the manuscript. This work was supported by the Ministry of Health and Welfare, Japan (S.U.), and a Grant-in-Aid for Scientific Research from the Ministry of Education, Science and Culture of Japan (S.U.).

Conflict of interest

We, the authors, declare that there were no conflicts of interest in conjunction with this paper.

References

1. Abe S, Usami S, Shinkawa H et al. Prevalent connexin 26 gene (*GJB2*) mutations in Japanese. J Med Genet 2000: 37: 41–43.
2. Ohtsuka A, Yuge I, Kimura S et al. *GJB2* deafness gene shows a specific spectrum of mutations in Japan, including a frequent founder mutation. Hum Genet 2003: 112: 329–333.
3. Park HJ, Hahn SH, Chun YM et al. Connexin26 mutations associated with nonsyndromic hearing loss. Laryngoscope 2000: 110: 1535–1538.
4. Liu XZ, Xia XJ, Ke XM et al. The prevalence of connexin 26 (*GJB2*) mutations in the Chinese population. Hum Genet 2002: 111: 394–397.
5. Wang YC, Kung CY, Su MC et al. Mutations of Cx26 gene (*GJB2*) for prelingual deafness in Taiwan. Eur J Hum Genet 2002: 10: 495–498.
6. Shi GZ, Gong LX, Xu XH et al. *GJB2* gene mutations in newborns with non-syndromic hearing impairment in Northern China. Hear Res 2004: 197: 19–23.

7. Dai P, Yu F, Han B et al. The prevalence of the c.235*del*C *GJB2* mutation in a Chinese deaf population. Genet Med 2007: 9: 283–289.
8. Kelley PM, Harris DJ, Comer BC et al. Novel mutations in the connexin 26 gene (*GJB2*) that cause autosomal recessive (DFNB1) hearing loss. Am J Hum Genet 1998: 62: 792–799.
9. Snoeckx RL, Huygen PL, Feldmann D et al. *GJB2* mutations and degree of hearing loss: a multicenter study. Am J Hum Genet 2005: 77: 945–957.
10. Cryns K, Orzan E, Murgia A et al. A genotype-phenotype correlation for *GJB2* (connexin 26) deafness. J Med Genet 2004: 41: 147–154.
11. Oguchi T, Ohtsuka A, Hashimoto S et al. Clinical features of patients with *GJB2* (connexin 26) mutations: severity of hearing loss is correlated with genotypes and protein expression patterns. J Hum Genet 2005: 50: 76–83.
12. Huculak C, Bruyere H, Nelson TN et al. V37I connexin 26 allele in patients with sensorineural hearing loss: evidence of its pathogenicity. Am J Med Genet 2006: 140: 2394–2400.
13. Denoyelle F, Marlin S, Weil D et al. Clinical features of the prevalent form of childhood deafness, DFNB1, due to a connexin-26 gene defect: implications for genetic counselling. Lancet 1999: 353: 1298–1303.
14. Lim LH, Bradshaw JK, Guo Y et al. Genotypic and phenotypic correlations of DFNB1-related hearing impairment in the Midwestern United States. Arch Otolaryngol Head Neck Surg 2003: 129: 836–840.
15. Iliadou V, Eleftheriades N, Metaxas AS et al. Audiological profile of the prevalent genetic form of childhood sensorineural hearing loss due to *GJB2* mutations in northern Greece. Eur Arch Otorhinolaryngol 2004: 261: 259–261.
16. Cohn ES, Kelley PM, Fowler TW et al. Clinical studies of families with hearing loss attributable to mutations in the connexin 26 gene (*GJB2*/DFNB1). Pediatrics 1999: 103: 546–550.
17. Yaeger D, McCallum J, Lewis K et al. Outcomes of clinical examination and genetic testing of 500 individuals with hearing loss evaluated through a genetics of hearing loss clinic. Am J Med Genet 2006: 140: 827–836.
18. Abe S, Yamaguchi T, Usami S. Application of deafness diagnostic screening panel based on deafness mutation/gene database using invader assay. Genet Test 2007: 11: 333–340.
19. Fuse Y, Doi K, Hasegawa T et al. Three novel connexin26 gene mutations in autosomal recessive non-syndromic deafness. Neuroreport 1999: 10: 1853–1857.
20. Brobby GW, Müller-Myhsok B, Horstmann RD. Connexin 26 R143W mutation associated with recessive nonsyndromic sensorineural deafness in Africa. N Engl J Med 1998: 338: 548–550.
21. Hişmi BO, Yilmaz ST, Incesulu A et al. Effects of *GJB2* genotypes on the audiological phenotype: variability is present for all genotypes. Int J Pediatr Otorhinolaryngol 2006: 70: 1687–1694.
22. Estivill X, Fortina P, Surrey S et al. Connexin-26 mutations in sporadic and inherited sensorineural deafness. Lancet 1998: 351: 394–398.
23. Kenna MA, Wu BL, Cotanche DA et al. Connexin 26 studies in patients with sensorineural hearing loss. Arch Otolaryngol Head Neck Surg 2001: 127: 1037–1042.
24. Wu BL, Lindeman N, Lip V et al. Effectiveness of sequencing connexin 26 (*GJB2*) in cases of familial or sporadic childhood deafness referred for molecular diagnostic testing. Genet Med 2002: 4: 279–288.
25. Yuge I, Ohtsuka A, Matsunaga T et al. Identification of 605ins46, a novel *GJB2* mutation in a Japanese family. Auris Nasus Larynx 2002: 29: 379–382.
26. Feng Y, He C, Xiao J et al. An analysis of a large hereditary postlingually deaf families and detecting mutation of the deafness genes. Lin Chuang Er Bi Yan Hou Ke Za Zhi. 2002: 16: 323–325.

Hearing Research 265 (2010) 90–95

Contents lists available at ScienceDirect

Hearing Research

journal homepage: www.elsevier.com/locate/heares

Research paper

Effect of vestibular labyrinth destruction on endocochlear potential and potassium concentration of the cochlea

Ryoukichi Ikeda *, Kazuhiro Nakaya, Muneharu Yamazaki, Takeshi Oshima, Tetsuaki Kawase, Toshimitsu Kobayashi

Department of Otolaryngology-Head & Neck Surgery, Tohoku University School of Medicine, 1-1 Seiryo-machi, Aoba-ku, Sendai 980-8574, Japan

ARTICLE INFO

Article history:
Received 25 November 2009
Received in revised form 18 December 2009
Accepted 22 December 2009
Available online 5 January 2010

Keywords:
Endocochlear potential
Semicircular canal
Potassium
Labyrinthectomy

ABSTRACT

Partial labyrinthectomy can result in maintenance of hearing under certain circumstances, and the mechanism of the hearing impairment caused by labyrinthectomy is unclear. We hypothesized that disruption of the membranous labyrinth results in electrical leakage and electrolyte imbalance. This study investigated the change in cochlear function by measurement of endocochlear potential (EP) and potassium concentration ($[K^+]$) caused by vestibular labyrinth destruction in the acute phase. Hartley guinea pigs underwent lateral semicircular canal (LSCC) transection with suctioning of the perilymph, ampullectomy, or destruction of the LSCC, superior SCC, and lateral part of the vestibule. The EP and $[K^+]$ were monitored using double-barreled ion-selective microelectrodes in the second turn of cochlea. The EP showed little to mild change after LSCC transectioning or ampullectomy, but declined variously and drastically after vestibulotomy. The EP did not recover but $[K^+]$ partially recovered after vestibulotomy. Disturbance of the mechanism of cochlear function caused by vestibular labyrinth destruction may involve reduction in the $[K^+]$ concentration in the endolymph.

1. Introduction

Surgical injury of the labyrinth is generally believed to result in complete hearing loss (Cawthorne, 1948). However, recent clinical experience and experimental studies have allowed surgical access to the inner ear with preservation of the cochlear function, thus providing a new gateway for the treatment of Ménière's disease (Yin et al., 2008), benign paroxysmal positional vertigo (Parnes and McClure, 1990), cholesteatoma (Kobayashi et al., 1995), skull base tumors (Hirsch et al., 1993), and acoustic neuromas (McElveen et al., 1991). Previous experimental reports support the idea that partial labyrinthectomy can result in maintenance of hearing. Mechanical trauma of the single semicircular canal in guinea pigs did not result in degeneration of the organ of Corti when examined by Preyer's reflexes (Kristensen, 1952, 1959). Auditory brain stem response (ABR) hearing thresholds were preserved after posterior semicircular canal occlusion in guinea pigs (Parnes and McClure, 1985). Transection of the lateral semicircular canal (LSCC) resulted in preservation of ABR thresholds, but removal of the semicircular canal ampulla in guinea pigs produced variable results, with some animals maintaining and others losing hearing, whereas widely opening the vestibule usually results in hearing loss (Smouha et al., 1996, 1999). Histological studies revealed early blind sac formation and late bony obliteration after transection and occlusion of the semicircular canal in guinea pigs (Nam et al., 1997, 2002).

We previously reported that endocochlear potential (EP) was preserved during extensive destruction of the semicircular canals of the guinea pig, whereas EP was lost by vestibulotomy (Kobayashi et al., 1991). The mechanism of the hearing impairment caused by labyrinthectomy is unresolved. Electrophysiologic changes, rather than cell death, may be responsible for the hearing loss after labyrinthectomy (Smouha et al., 1996). The high positive EP (80–90 mV) results from the unique ionic composition of the cochlear endolymph with a high potassium concentration ($[K^+]$: ~150 mM), and is essential for the excitation of the hair cells that are the basis of hearing (Konishi et al., 1978). Therefore, we hypothesized that disruption of the membranous labyrinth could result in electrical leakage and electrolyte imbalance.

The present study investigated the mechanism of acute phase change in cochlear function caused by vestibular labyrinth destruction by measurement of EP and $[K^+]$.

Abbreviations: $[K^+]$, potassium concentration; EP, endocochlear potential; LSCC, lateral semicircular canal; SSCC, superior semicircular canal; ABR, auditory brain stem response

* Corresponding author. Tel.: +81 22 717 7304; fax: +81 22 717 7307.
E-mail address: ryoukich@hotmail.com (R. Ikeda).

0378-5955/$ - see front matter © 2009 Elsevier B.V. All rights reserved.
doi:10.1016/j.heares.2009.12.027

2. Materials and methods

2.1. Animal preparation

Male Hartley guinea pigs, weighing between 200 and 250 g, were anesthetized by intraperitoneal injection of 40 mg/kg ketamine and 10 mg/kg xylazine, and spontaneous breathing was maintained with room air through a tracheal cannula. Additionally, 1% lidocaine was infiltrated into the surgical area for local anesthesia before the surgery. Animal pain responses were monitored during the procedures, and additional anesthetic was administered as needed. Four or five animals were used in each of three experimental surgery groups. The Animal Care and Ethics Committee of Tohoku University Graduate School of Medicine approved all experimental protocols.

2.2. Measurement of EP and K^+

The endolymphatic [K^+] and the EP were measured using double-barreled K^+-selective electrodes. All measurements were made in the second cochlear turn after thinning the bone over the stria vascularis and forming a small hole. The methods used to fabricate the ion-sensitive, double-barreled electrodes were described previously (Nakaya et al., 2007). Double-barreled glass microelectrodes were manufactured from filament-containing glass tubing (1B100F-4; World Precision Instruments, Sarasota, FL) using a micropipette puller (PD-5; Narishige Group, Tokyo, Japan). The two capillaries were gently rotated through 180° along the longitudinal axis by heating, to fix the tips of the two pipettes, and then pulled. Before silanization, the microelectrodes were heated at 200 °C for 2 h to ensure dryness. The longer ion-selective barrel was mounted in the lid of a beaker. The beaker was heated to 200 °C and silanized by a 90-s exposure to 0.02 ml dimethyldichlorosilane (Fluka 40136; Fluka Chemical, Ronkonkoma, NY). The shorter reference barrel was protected from silanization by sealing the open end with Parafilm (PM-992; American National Can, Menasha, WI). After silanization, the microelectrodes were heated at 200 °C for 2 h. The EP was recorded simultaneously from the reference barrel of the electrode. The reference barrel was filled with 500 mM NaCl solution and the ion barrel was filled with 1 M KCl. A Fluka 60398 exchanger was used for this electrode (Fluka Chemical). All electrodes were calibrated before and after use in three standard solutions containing 15, 47.5, and 150 mM KCl at 37 °C. Signals were amplified by an FD223a Electrometer (World Precision Instruments, New Haven, CT), converted by an analog-to-digital converter (Power Lab/4s; Power Lab, Gladstone, Australia), and then stored digitally on a hard disk. Each barrel was connected to an input of a grounded dual electrometer (FD223a; World Precision Instruments) via Ag–AgCl wire electrodes. The animal was grounded via an Ag–AgCl wire electrode inserted under the skin at the abdomen.

2.3. Surgery

Surgery was begun with a retroauricular skin incision. The epitympanic bulla was opened by drilling a burr hole approximately 2 mm directly superior to the external canal. The individual procedures performed were as follows.

2.3.1. LSCC transection with suctioning of perilymph (four animals)

The tympanic bulla was enlarged posteriorly, the ridge of bone was drilled down superior and posterior to the facial nerve, and the lumen of the LSCC was identified and drilled for 0.4 mm in a single location. After fluid was visualized exiting the holes, suction was used gently through filament-containing glass tubing (1B100F-4; World Precision Instruments, Sarasota, FL) and held for 5 min. The tips of the glass tubing were cut to 0.2 mm outer diameter.

2.3.2. Ampullectomy (four animals)

The labyrinth was approached via the tympanic bulla directly above the external canal, and the LSCC ampullae were identified and opened. As only a slight shift caused by the ampullectomy maneuver would destroy the ion-selective electrode inserted in the cochlea, EP and [K^+] could not be reliably measured during this period. Therefore, we inserted the double barrel electrodes after the surgery. The measurement was made about 3 min after destruction of the ampulla.

2.3.3. Vestibulotomy (five animals)

The LSCC and SSCC ampullae were drilled out. Drilling of the vestibule was continued until a hole twice the size of the LSCC ampullae was made. Care was taken not to damage the membranous labyrinth excessively. Recordings of EP and [K^+] were similar to those for ampullectomy.

2.4. Statistical methods

EP and [K^+] data was statistically analyzed to determine significance. Differences were determined by unpaired *t*-test. Significance was assumed at $P < 0.05$.

3. Results

LSCC transection and suctioning for 5 min showed little change in the EP or the [K^+] recorded in the second cochlear turn. During surgery, the EP was almost stable and [K^+] was elevated slightly (Fig. 1). Before surgery in the normal condition, EP was 79.00 ± 1.71 mV ($n = 4$) and [K^+] was 155.28 ± 8.49 mM ($n = 4$). After surgery, EP and [K^+] finally reached 73.95 ± 7.33 mV ($n = 4$) and 174.08 ± 6.26 mM ($n = 4$).

Ampullectomy resulted in EP of 80.48 ± 8.17 mV ($n = 4$), but [K^+] declined immediately and eventually recovered to 169.38 ± 6.89 mM ($n = 4$) (Fig. 2). The results showed no significant difference between LSCC transection and ampullectomy in the final state of EP and [K^+].

Vestibulotomy caused EP to drastically decline without recovery to 49.08 ± 15.06 mV ($n = 5$) (Fig. 3). [K^+] also declined abruptly and gradually increased to 143.4 ± 14.22 mM ($n = 5$), but never completely returned to the original level, and the individual results were more variable than those of LSCC transection and ampullectomy. These changes were significantly different to those induced by LSCC transection and ampullectomy (Fig. 4).

4. Discussion

The present study demonstrated that LSCC destruction without suctioning and ampullectomy caused little to mild change in EP, whereas vestibulotomy caused drastic decline in EP which did not recover, and decrease in [K^+] which partially recovered.

LSCC destruction without suctioning resulted in hearing preservation in ABR (Parnes and McClure, 1985; Smouha et al., 1996, 1999) and EP of the first cochlear turn (Kobayashi et al., 1991). Interruption of the duct of the LSCC hardly altered the N1 input–output function curve during the 1-h observation period in acoustic neuroma patients (Kobayashi et al., 1991). Individual cases of incidental hearing preservation following injury to the LSCC have been reported in patients following fenestration surgery for otosclerosis (Cawthorne, 1948) and chronic otitis media (Palva et al., 1976). Based on these reports, several innovative inner ear surgical procedures have been developed.

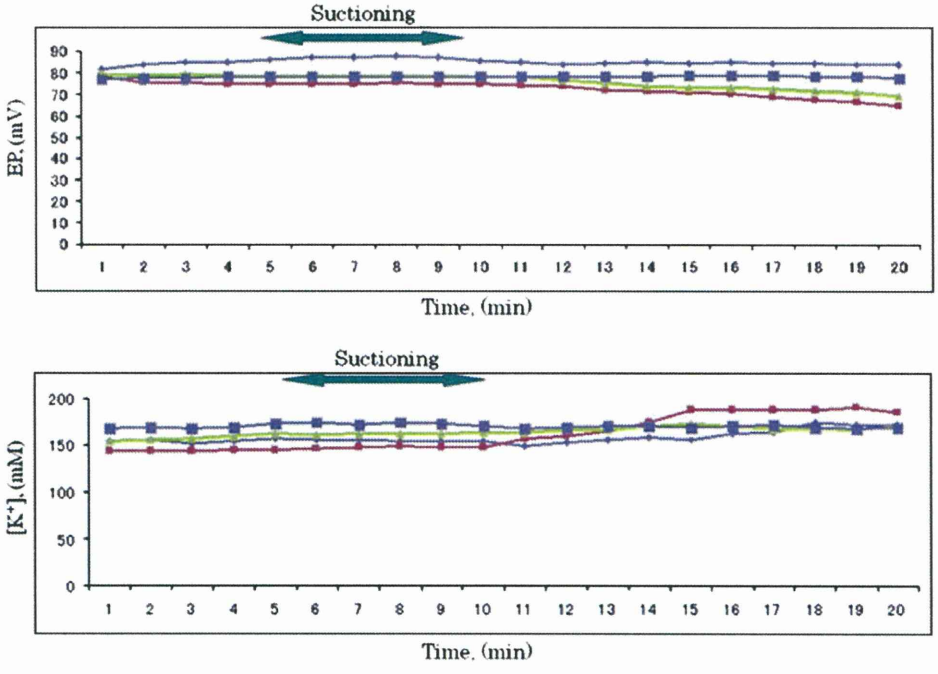

Fig. 1. Changes in the EP and [K^+] recorded in the second cochlear turn during interruption and suctioning for 5 min of the lateral semicircular canal ($n = 4$). Each line represents data from one animal.

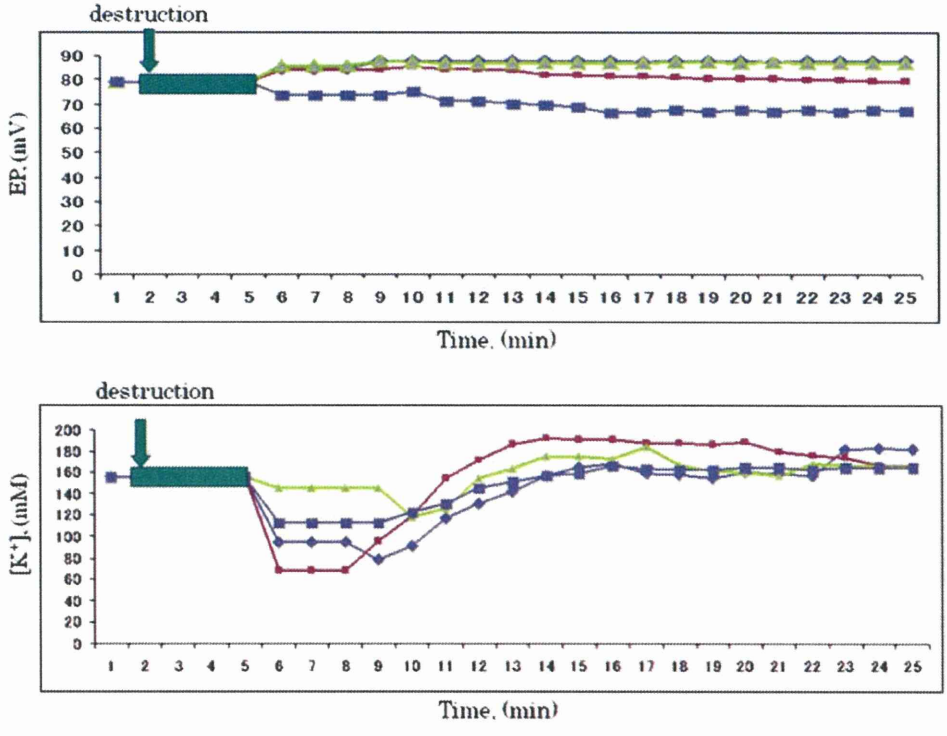

Fig. 2. Changes in the EP and [K^+] recorded in the second cochlear turn during destruction of the lateral semicircular canal ampulla ($n = 4$).

Previously, LSCC transection and suctioning of inner ear fluid led to a transient loss of hearing measured with ABR although thresholds eventually recovered in the guinea pig (Smouha et al., 1999). This contradiction may be explained by the different techniques used, as the previous study used a No. 3 Baron suction device held directly between two holes for 5 min, whereas we transected and suctioned only one location and the suction instrument had a smaller diameter. Our results showed that slight suctioning of inner ear fluid in semicircular canal resulted in preserved hearing in the guinea pig. Guinea pigs differ significantly from humans in the smaller diameter of the bony labyrinth and the patency of the cochlear aqueduct. The patent cochlear aqueduct is

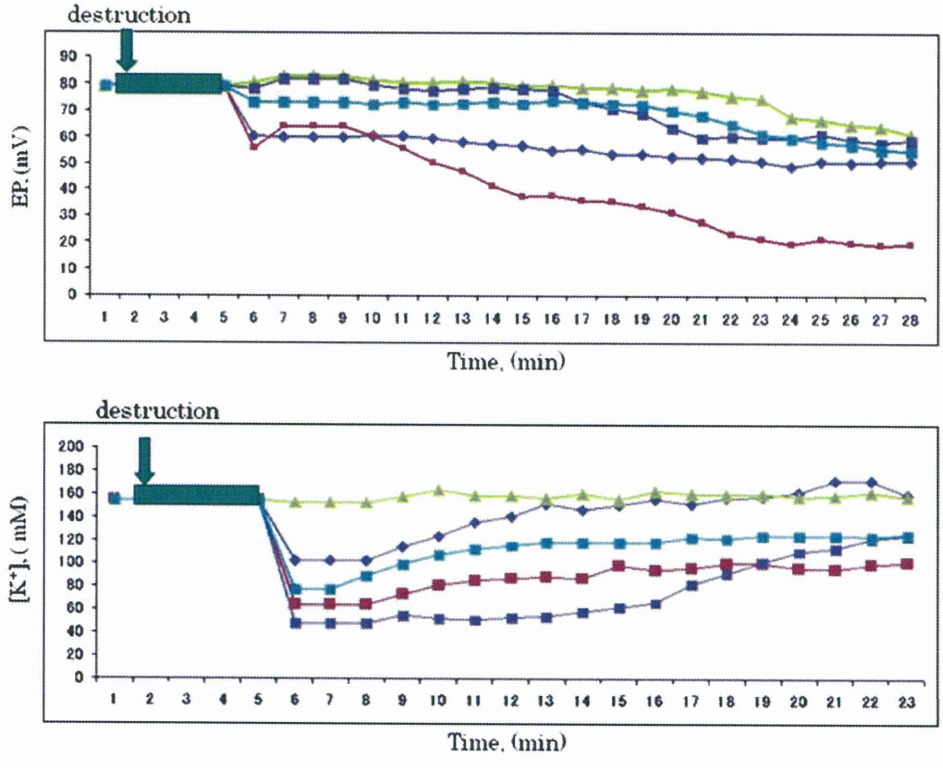

Fig. 3. Changes in the EP and [K^+] recorded in the second cochlear turn during destruction of the vestibule ($n = 5$).

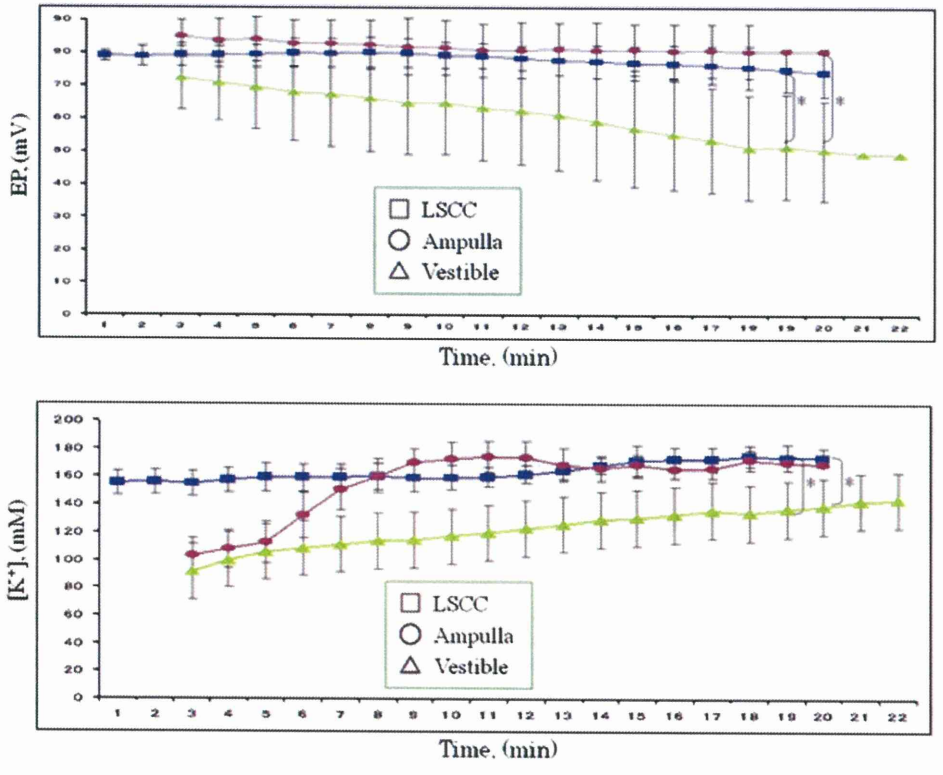

Fig. 4. Mean changes in the EP and [K^+] during LSCC transection and suctioning, ampullectomy, and vestibulotomy. Significant differences are marked ($^*P < 0.05$). Bars indicate the standard deviations calculated at 1 min intervals.

important in the replacement of lost perilymph, and cerebrospinal fluid can flow from the subarachnoid space into the perilymphatic space in the guinea pig (Moscovitch et al., 1973). In contrast, the cochlear aqueduct is often constricted and sometimes obstructed in humans (Rask-Andersen et al., 1977). Other routes, such as the perivascular and perineural at the modiolus, may compensate for

loss of perilymph. Ampullectomy resulted in hearing preservation, which is consistent with previous findings (Smouha et al., 1996, 1999).

Entry of the vestibule caused significant EP decline without complete loss of cochlear function. These findings paralleled other observations in animals and humans. Wide vestibulotomy led to permanent, incomplete loss of hearing recorded by click-evoked ABR (Smouha et al., 1996), tone-burst ABR (Smouha et al., 1999), and EP (Kobayashi et al., 1991) in the guinea pig. In addition, these individual results were variable. Vestibulotomy had a variable effect on hearing thresholds, with permanent partial hearing loss that was moderate in some subjects and severe in others. Therefore, entering the inner ear at or near the vestibule results in varying degrees of damage to the membranous labyrinth and to the cochlea (Smouha et al., 1999). Furthermore, the membranous labyrinth is very difficult to identify precisely in vestibulotomy under a light microscope, so these inconsistent results including our study may be due to the variable extent of damage of the utricle and the saccule which is impossible to quantify. Intrusion into the vestibule led to intraoperative hearing loss, as measured by ABR, suggesting that maintaining fluid in the vestibule is important for hearing preservation. Several factors seem important for hearing preservation (McElveen et al., 1993). The semicircular canals have narrow body canal lumens, and are located far from the cochlea. The endolymphatic valve in the utricle has a protective function, which may prevent excessive loss of perilymph during surgery (Schuknecht and Belal, 1975). Occlusion following transection of the LSCC in the guinea pig formed blind ducts in the membranous endolymphatic canal. Interruption of the communication between the endolymph and perilymph as quickly as possible seems to be important in preserving postoperative hearing (Nam et al., 2002). There seems to be no effective means to prevent intralabyrinthine communication following a saccular or utricular rupture in the vestibule.

Recently, the "pools" concept of endolymph homeostasis was proposed (Salt, 2001). Endolymphatic compartments are represented by a number of pools (endolymphatic sac, saccule, and cochlea) connected by small ducts (endolymphatic duct and ductus reuniens). Flow between the compartments occurs as needed to balance the levels of the individual pools. Small volume changes of less than 5 nl/min are corrected locally, without inducing longitudinal flow in the cochlea. Increases or decreases of cochlear endolymph volume beyond the capacity of local mechanisms result in substantial longitudinal volume flows. Local volume regulation processes in the saccule or other vestibular structures have not been demonstrated, but are possible.

The EP is generally understood to originate in the stria vascularis and to provide the main driving force for sensory transduction (Wangemann et al., 1996). K^+ is important in the cochlea. K^+ is the major cation in the endolymph, and is the charge carrier for sensory transduction and generation of the EP (Wangemann, 2006).

Vestibular dark cells in the ampulla secrete K^+ into endolymph by mechanisms similar to those found in strial marginal cells (Wangemann, 1995), although cycling is not associated with the generation of a large voltage equivalent to the EP. K^+ in the vestibular endolymph flows into the vestibular hair cells via the transduction channel and is released via KCNQ4 and other K^+ channels in the basolateral membrane (Griguer et al., 1993). Vestibular dark cells release K^+ into endolymph via the K^+ channel KCNQ1/KCNE1 in the apical membrane. Mice lacking KCNJ10 are deaf but appear to maintain normal vestibular function, consistent with the finding that KCNJ10 is expressed in the cochlea but not the vestibular labyrinth (Hibino et al., 1997; Marcus et al., 2002). The endolymphatic $[K^+]$ in the utricle of mice lacking the KCNJ10K^+ channel was not different from that in wild-type mice (Marcus et al., 2002).

This study showed that $[K^+]$ declined abruptly and recovered gradually after ampullectomy and vestibulotomy. Strong mechanical disturbance of the membranous labyrinth resulted in mixing of the perilymphatic and endolymphatic fluids. The destruction area of vestibulotomy was wider than that of ampullectomy, so $[K^+]$ after vestibulotomy declined suddenly and never completely returned to the original levels. In addition, the dark cells in the utricle cover almost the entire posterior wall and the periphery of the anterior wall, and in the ampullae at the base of the cristae on the canal side, so the K^+ channels in these areas were interrupted. After LSCC destruction with suctioning, $[K^+]$ showed little change because only the ampulla contains the dark cells in the semicircular canal (Oudar et al., 1988) and is the site of endolymph secretion (Bernard et al., 1986).

In conclusion, the inner ear of guinea pigs is capable of withstanding surgical trauma to the semicircular canals, ampulla, and vestibule without suffering complete loss of cochlear function. Furthermore, vestibule destruction had a variable effect on EP. Destruction of the vestibule causes the greatest damage to the membranous labyrinth among the three procedures. Torn membrane also gives rise to mixtures of endolymph and perilymph, and loss of K^+ in the endolymph. The $[K^+]$ declines abruptly and recovers gradually after ampullectomy and vestibulotomy. Disturbance of the mechanism of cochlear function caused by vestibular labyrinth destruction may involve reduction in the K^+ concentration in the endolymph.

Acknowledgement

This study was supported by a grant from the Ministry of Education, Science and Culture [Grant-in-Aid for Scientific Research (B) 21390457].

References

Bernard, C., Ferrary, E., Sterkers, O., 1986. Production of endolymph in the semicircular canal of the frog *Rana esculenta*. J. Physiol. 371, 17–28.
Cawthorne, T., 1948. The effect on hearing in man of removal of the membranous lateral semicircular canal. Acta Otolaryngol. Suppl. 78, 145–149.
Griguer, C., Sans, A., Lehouelleur, J., 1993. Non-typical K(+)-current in cesium-loaded guinea pig type I vestibular hair cell. Pflugers Arch. 422, 407–409.
Hibino, H., Horio, Y., Inanobe, A., Doi, K., Ito, M., Yamada, M., Gotow, T., Uchiyama, Y., Kawamura, M., Kubo, T., Kurachi, Y., 1997. An ATP-dependent inwardly rectifying potassium channel, KAB-2 (Kir4.1), in cochlear stria vascularis of inner ear: Its specific subcellular localization and correlation with the formation of endocochlear potential. J. Neurosci. 17, 4711–4721.
Hirsch, B., Cass, S.P., Sekhar, L., Wright, D.C., 1993. Translabyrinthine approach to skull base tumors with hearing preservation. Am. J. Otolaryngol. 14, 533–543.
Kobayashi, T., Sato, T., Toshima, M., Ishidoya, M., Suetake, M., Takasaka, T., 1995. Treatment of labyrinthine fistula with interruption of the semicircular canals. Arch. Otolaryngol. Head Neck Surg. 121, 469–475.
Kobayashi, T., Shiga, N., Hozawa, K., Hashimoto, S., Takasaka, T., 1991. Effect on cochlear potentials of lateral semicircular canal destruction. Arch. Otolaryngol. Head Neck Surg. 117, 1292–1295.
Konishi, T., Hamrick, P.E., Walsh, P.J., 1978. Ion transport in guinea pig cochlea. I. Potassium and sodium transport. Acta Otolaryngol. 86, 22–34.
Kristensen, H.K., 1952. Acoustic and vestibular function in guinea-pigs after removal of the membranous external semicircular canal. J. Laryngol. Otol. 66, 259–275.
Kristensen, H.K., 1959. Acoustic-vestibular and histologic examinations in guinea-pigs after interruption of membranous labyrinth in semicircular canals or cochlea. J. Laryngol. Otol. 73, 699–721.
Marcus, D.C., Wu, T., Wangemann, P., Kofuji, P., 2002. KCNJ10 (Kir4.1) potassium channel knockout abolishes endocochlear potential. Am. J. Physiol. 282, C403–C407.
McElveen Jr., J.T., Wilkins, R.H., Erwin, A.C., Wolford, R.D., 1991. Modifying the translabyrinthine approach to preserve hearing during acoustic tumour surgery. J. Laryngol. Otol. 105, 34–37.
McElveen Jr., J.T., Wilkins, R.H., Molter, D.W., Erwin, A.C., Wolford, R.D., 1993. Hearing preservation using the modified translabyrinthine approach. Otolaryngol. Head Neck Surg. 108, 671–679.
Moscovitch, D.H., Gannon, R.P., Laszio, C.A., 1973. Perilymph displacement by cerebrospinal fluid in the cochlea. Ann. Otol. Rhinol. Laryngol. 82, 53–61.
Nakaya, K., Harbidge, D.G., Wangemann, P., Schultz, B.D., Green, E.D., Wall, S.M., Marcus, D.C., 2007. Lack of pendrin HCO_3^- transport elevates vestibular

endolymphatic [Ca^{2+}] by inhibition of acid-sensitive TRPV5 and TRPV6 channels. Am. J. Physiol. Renal Physiol. 292, F1314–F1321.
Nam, B.H., Park, C.I., Jung, T.T., 2002. Early histopathologic changes after lateral semicircular canal transection and occlusion in guinea pigs. Ann. Otol. Rhinol. Laryngol. 111, 402–406.
Nam, B.H., Yoon, S.K., Park, C.I., 1997. Transection and occlusion of lateral semicircular canal in guinea pigs. Ann. Otol. Rhinol. Laryngol. 106, 1082–1086.
Oudar, O., Ferrary, E., Feldmann, G., 1988. Ultrastructural study of the semicircular canal cells of the frog *Rana esculenta*. Anat. Rec. 220, 328–334.
Palva, T., Kärjä, J., Palva, A., 1976. Immediate and short-term complications of chronic ear surgery. Arch. Otolaryngol. 102, 137–139.
Parnes, L.S., McClure, J.A., 1985. Effect on brainstem auditory evoked responses of posterior semicircular canal occlusion in guinea pigs. J. Otolaryngol. 14, 145–150.
Parnes, L.S., McClure, J.A., 1990. Posterior semicircular canal occlusion for intractable benign paroxysmal positional vertigo. Ann. Otol. Rhinol. Laryngol. 99, 330–334.
Rask-Andersen, H., Stahle, J., Wilbrand, H., 1977. Human cochlear aqueduct and its accessory canals. Ann. Otol. Rhinol. Laryngol. Suppl. 86 (5 Pt. 2 Suppl. 42), 1–16.
Salt, A.N., 2001. Regulation of endolymphatic fluid volume. Ann. NY Acad. Sci. 942, 306–312.
Schuknecht, H.F., Belal, A.A., 1975. The utriculo-endolymphatic valve: its functional significance. J. Laryngol. Otol. 89, 985–996.
Smouha, E.E., Inouye, M., Sobol, L.L., Slepecky, N.B., 1999. Histologic changes after semicircular canal occlusion in guinea pigs. Am. J. Otol. 20, 632–638.
Smouha, E.E., Namdar, I., Michaelides, E.M., 1996. Partial labyrinthectomy with hearing preservation: an experimental study in guinea pigs. Otolaryngol. Head Neck Surg. 114, 777–784.
Wangemann, P., 1995. Comparison of ion transport mechanisms between vestibular dark cells and strial marginal cells. Hear. Res. 90, 149–157.
Wangemann, P., Shen, Z., Liu, J., 1996. K(+)-induced stimulation of K^+ secretion involves activation of the IsK channel in vestibular dark cells. Hear. Res. 100, 201–210.
Wangemann, P., 2006. Supporting sensory transduction: cochlear fluid homeostasis and the endocochlear potential. J. Physiol. 576, 11–21.
Yin, S., Chen, Z., Yu, D., Wu, Y., Shi, H., Zhou, H., Wang, J., 2008. Triple semicircular canal occlusion for the treatment of Ménière's disease. Acta Otolaryngol. 128, 739–743.